KINGFA
INNOVATION CHANGE LIFE

Recycled PET foaming: Supercritical carbon dioxide assisted extrusion with real-time quality monitoring

Katalin Bocz [a], Ferenc Ronkay [b, c], Béla Molnár [b, c], Dániel Vadas [a], Martin Gyürkés [a], Dániel Gere [b, c], György Marosi [a], Tibor Czigany [c, d, *]

[a] Department of Organic Chemistry and Technology, Faculty of Chemical Technology and Biotechnology, Budapest University of Technology and Economics, Műegyetem rkp. 3., H-1111 Budapest, Hungary
[b] Imsys Ltd, Material Testing Laboratory, Mozaik Street 14/A., H-1033 Budapest, Hungary
[c] Department of Polymer Engineering, Faculty of Mechanical Engineering, Budapest University of Technology and Economics, Műegyetem rkp. 3., H-1111 Budapest, Hungary
[d] MTA-BME Research Group for Composite Science and Technology, H-1111 Budapest, Muegyetem rkp. 3., H-1111 Budapest, Hungary

ARTICLE INFO

ABSTRACT

Foaming of recycled poly(ethylene terephthalate) (rPET) was performed by supercritical carbon dioxide (sc-CO_2) assisted extrusion. The intrinsic viscosity (IV) of rPET was increased from 0.62 dl/g to 0.87 dl/g using an epoxy-functional chain extender, which provided adequate rheological properties for cell stabilization so that an apparent density of less than 0.15 g/cm^3 became achievable. Homogeneous and talc induced heterogeneous crystal and cell nucleation, subsequent cell growth and stabilization processes were examined using differential scanning calorimetry (DSC) and scanning electron microscopy (SEM), respectively. It was found that using talc the crystallization temperature increases which results in smaller cell size distribution. A strong correlation was evinced between the apparent density and the Fourier transform near-infrared (NIR) spectrum of the foamed rPET samples enabling quick and non-destructive characterization. Accordingly, NIR spectroscopy is demonstrated as a suitable method for in-line quality monitoring during extrusion foaming of recycled PET, being especially prone to quality fluctuations.

1. Introduction

Industrial development poses a number of new challenges for plastic processing. Important tasks are to continuously ensure the quality of the products, to develop the flexibility of the production processes, and to increase the efficiency of production. In addition to the introduction of Industry 4.0, for sustainable development, the aspects of the circular economy must also be taken into account, in which the high-level recycling of used plastic products is an important pillar [1]. The recent crisis caused by the coronavirus (SARS-CoV-2) has led to the closure of many community meeting and dining venues, resulting in increased consumption of retail food and more frequent home delivery, and thereby a rapid rise in single-use plastic packaging and their waste [2]. In the case of thermoplastic polymers, recycling can be efficiently realized physically by melt processing after the collection and purification of the selectively collected or separated discarded products [3].

Poly(ethylene terephthalate) (PET) is one of the most commonly used thermoplastics in the world, an annual volume of 19 million tons is produced for short-lived packaging [4]. These typical bottle products usually appear in the waste stream even in the year of manufacture [5], or in the worst case due to irresponsible human behaviour in the environment [6], causing significant environmental impact [7]. After proper collection, sorting, washing, and purification, recycling is possible, but this process is hampered by the degradation of the molecular chains. In addition to UV radiation on products [8,9], hydrolytic and thermal degradation during processing are primarily responsible for the shortening of the molecular chains [10,11]. Degradation reduces the melt viscosity of the

material [12—14], which can cause processing difficulties. The aesthetic and functional mechanical properties of the produced secondary raw material or products are also negatively affected by degradation [15,16]. In the case of PET, the average length of the molecular chains is generally characterized by the intrinsic viscosity value determined by solution viscosity [17]. The intrinsic viscosity value of the original raw material used for bottle production is usually in the range of 0.78—0.82 dl/g [18], but during processing this value can also decrease by 0.06—0.08 dl/g.

Involving foaming in the recycling process can provide an opportunity to produce new, even longer-lasting products that can be used for heat and sound insulation purposes, e.g. in the field of construction. In this field, it is advantageous that thermoplastic PET foam products can be physically recycled after use, as opposed to crosslinked foams (e.g. polyurethane). This application area requires the production of suitably low-density, uniform-quality, homogeneous foams by a productive process. Low density can be achieved primarily with physical blowing agents (PBAs) (e.g. N_2 or CO_2 gas or supercritical fluid), the appropriate cell density and cell size distribution are mainly from nucleating agents (e.g. include calcium carbonate, calcium stearate, magnesium silicate, the mixture of citric acid and sodium bicarbonate, rubber particles, sodium benzoate, stearic acid, silica products, talc, and zinc stearate), technological parameters (temperature, pressure) and characteristics of the polymer (e.g. molecular weight, branching) [19,20]. External particles or surfaces work as heterogeneous nucleating sites during foaming [21]. The heterogeneous nucleation decreases the energy-barrier dramatically for cell nucleation, increases the nucleation rate, and is expected to narrow the cell size distribution [22]. Productivity is best provided by extrusion foaming, which has significantly higher yields than batch foaming, compression moulding, or even injection moulding.

Extrusion foaming with supercritical CO_2 (sc-CO_2) enables the manufacturing of products with very light (ρ = 3—50 kg/m^3) apparent density [23,24]. The purposeful process consists of three parts: in the first step, liquid CO_2 is introduced into the polymer melt under high pressure, where rapid mixing and dissolution of the in—situ formed supercritical sc-CO_2 in the polymer melt occur. This step takes place in the extruder, where a saturation concentration is reached under the given conditions. In addition to temperature and pressure conditions, saturation is also affected by gas solubility and residence time. In the second step, the polymer/gas solution exits the die, during which there is a sudden pressure drop, which drastically reduces the solubility of the gas and results in phase separation. This is the cell nucleation step that determines the resulting cell density. The third step is cell growth, which lasts until it is hindered by opposing forces resulting from the viscosity of the matrix. The resulting cell size is determined by the cooling and pressure conditions, the concentration of gas dissolved in the melt, and the viscoelastic properties of the matrix [25]. If the viscosity of the matrix is inadequate, the cells may coalesce and/or collapse during growth, which significantly impair the resulting density [26].

Foaming of recycled PET has been the focus of research since the mid-1990s due to the increasing amount of waste generated and the new advances in molecular weight increasing processes. The quality of the raw materials used in the research, the technology used, and the average cell size achieved, as well as the apparent density, are summarized in Table 1. It can be stated that a lower apparent density can be achieved with physical foaming than with chemical foaming, which can be mainly explained by the higher cell density characterizing the nucleation behaviour. It can also be observed that with the batch technology of the physical processes, a density of less than 0.1 g/cm^3 is achievable, which can be

explained by the significantly longer diffusion time compared to extrusion technology.

The viscoelastic properties of the polymer melt play an important role in the resulting cell distribution of the foam product. Several have shown that methods that create chain branches significantly increase melt elasticity and increase relaxation time compared to linear chain lengthening, which also helps prevent cell fusion, thereby making cell growth more stable [26—30].

Methods that are commonly used for the qualification and quality control of the structure of foams are either batch procedures, performed with samples taken from production, or in-line applicable during continuous production. The advantage of in-line measurements is that the quality of the foamed products can be monitored in real time and preferably in a non-destructive way. If there is a change in the tested characteristic, it is possible to immediately change the production parameters (e.g. zone temperature, pressure, screw speed, CO_2 flow rate) through signal processing and feedback, so that in-line control can be established. An in-line FT-NIR measurement system for co-extrusion foaming technology was developed by Nagata et al. and successfully used to determine the CO_2 concentration in the polymer [31,32]. Tatibouet et al. used an in-line ultrasonic technique, built into the extruder to determine the onset of phase separation in the polymer melt [33,34]. Common et al. used Raman spectroscopy to characterize residence time and mixing during extrusion foaming [35].

The aim of the present research was to develop recycled PET raw materials using chain extender and nucleating additives that can be used to produce low-density (microcellular) foams. Based on literary antecedents (Table 1), by processing PET recyclates with typical intrinsic viscosity values of 0.70—0.90 dl/g using the industrially more relevant extrusion foaming technology, the achievable foam density is limited to the range of 0.8—0.9 g/cm^3. An exeption is our previous study, where foams with density of 0.24 g/cm^3 were produced by sc-CO_2 assisted extrusion using PET bottle regrinds with an intrinsic viscosity of 0.74 dl/g as starting material [29]. In this work, our extrusion technology has been further developed, and not only to achieve lower apparent densities, but to create and validate an in-line applicable non-destructive measurement procedure for continuous quality (density) control of the recycled foams, being especially prone to quality fluctuations.

2. Materials and methods

2.1. Materials

PET bottle flakes (Jász-Plasztik Ltd., Hungary), originating from collected, washed, and sorted post-consumer PET bottles, with an intrinsic viscosity value of 0.73 dl/g were used as matrix material. As nucleating agent, HTPultra5 L type talc (IMI FABI SpA, Italy), with a median particle diameter of 0.65 μm was used. To increase melt viscosity and intrinsic viscosity, a styrene-acrylic oligomer multifunctional epoxide chain extender, Joncryl ADR 4468 (BASF SE, Germany) with a molecular weight of 7250 g/mol and an epoxy equivalent weight of 310 g/mol [50,51] (specific gravity: 1.08 g/cm^3; glass transition temperature: 54 °C) was used.

2.2. Methods

The rPET flakes were dried for 4 h at 160 °C, before compounding. LTE 26—44 (Labtech Engineering, Thailand) twin-screw extruder was used for the mixing with zone temperatures between 245 and 260 °C.

Intrinsic viscosity value was used for characterisation of the average molecular weight. The relation between the intrinsic

Table 1
Summary of recent result in the field of PET and recycled PET foaming (PBA: physical blowing agent, CBA: chemical blowing agent).

Initial intrinsic viscosity [dl/g]	Chain extender additive or process	Modified intrinsic viscosity [dl/g]	Foaming technology	Type of foaming agent	Apparent density [g/cm³]	Average cell diameter [μm]	Cell density [cells/cm³]	Year	Reference
0.83	–	–	batch	PBA	no data	2	$4.4*10^{11}$	1995	Baldwin et al. [36]
no data	no data	1.20	extrusion	CBA	0.80	65	no data	1998	Xanthos et al. [27]
0.78	tetrafunctional epoxy	no data	batch	PBA	0.09	60	no data	2000	Japon et al. [37]
no data	PMDA	0.95	extrusion	PBA	0.20	270	no data	2000	Xanthos et al. [38]
no data	–	–	compression moulding	CBA	0.82	52	$8*10^{6}$	2004	Guan et al. [39]
0.74	PMDA	no data	extrusion	CBA	1.17	50	$1.2*10^{6}$	2005	Maio et al. [40]
0.49	PMDA	0.77	extrusion	CBA	0.90	37	$2.9*10^{5}$	2009	Coccorullo et al. [41]
1.25	–	–	batch	PBA	0.06	25	10^{8}	2010	Sorrention et al. [42]
0.67	PMDA	0.88	batch	PBA	0.03	30	$1.5*10^{9}$	2014	Xia et al. [43]
0.8	tetrafunctional epoxy	no data	batch	PBA	0.07	86	no data	2014	Liu et al. [44]
0.70	multifunctional epoxide + solid state polycondensation	1.14	batch	PBA	0.09	30	$5.4*10^{8}$	2015	Yan et al. [28]
–	modified polymerization by pentaerythritol (PENTA) + solid state polycondensation	1.5	extrusion	PBA	0.14	265	$4.6*10^{5}$	2016	Fan et al. [30]
0.65	–	–	injection moulding	CBA	1.16	95	no data	2017	Ronkay et al. [45]
0.76	PBT-glycidyl methacrylate-styrene copolymer	0.95	batch	PBA	no data	61	$1.8*10^{8}$	2017	Li et al. [46]
0.8	multifunctional epoxide	no data	injection moulding	CBA	1.17	100	no data	2019	Szabó and Dogossy [47]
no data	multifunctional epoxide	0.96	extrusion	CBA	0.88	148	no data	2019	Lai et al. [48]
0.71	multifunctional epoxide	0.74	extrusion	PBA	0.24	219	no data	2019	Bocz et al. [29]
no data	–	–	extrusion	PBA	0.20	400	$8*10^{4}$	2020	Yao et al. [49]

viscosity and average molecular weight is described by the Mark–Houwink's Equation (1) [52]:

$$[\eta] = KM^{\alpha} \tag{1}$$

where $[\eta]$ is the solution intrinsic viscosity, M is the average molecular weight, and K and α are constants that are specific for fixed conditions of polymer type, solvent and temperature.

The intrinsic viscosity of the base material and the specimens was determined using a computer-controlled PSL Rheotek automatic solution viscometer equipped with an optical sensor. Phenol-tetrachloroethane mixture in the ratio of 60:40% was applied as a solvent, concentration was 0.5 g/dl, and examination temperature was 30 °C. Two parallel measurements were performed in all cases.

Melt rheology under dynamical shear was investigated using an AR 2000 type rotational rheometer (TA Instruments, New Castle, DE, USA) with 25 mm diameter parallel-plate geometry. Dynamic frequency sweep tests were performed at 260 °C in nitrogen atmosphere to measure the complex shear viscosity over a frequency range of 0.1–100 Hz.

Prior to foaming, the regranulates were dried at 160 °C for 4 h. Sc-CO₂ assisted extrusion foaming was carried out on a modified Collin Teach-Line ZK 25T type co-rotating twin-screw extruder (Dr Collin GmbH, Ebersberg, Germany) with a screw diameter of 25 mm and an L/D ratio of 24. The extruder has 5 heating zones: 1–3. zone plasticizing and melt transport section; the sc-CO₂ is introduced into the 4. zone using a syringe pump (Teledyne Isco 260D, Lincoln, NE, USA). This is followed by the last (zone 5) of the extruder, followed by the melt pump and the static mixer, which ensure even, homogeneous mixing and material flow. The temperature of these elements and the pressure drop across them were continuously monitored. The die had a circular cross-section with an opening of 2 mm in diameter. The continuously exiting foamed products were collected using a conveyor and cooled in the air.

NIR spectra were collected using a Bruker Optics MPA™ FT-NIR spectrograph (Bruker Optik GmbH, Ettlingen, Germany) equipped with a Solvias fiber optic probe (Solvias AG, Kaiseraugust, Switzerland) in reflection mode. The instrument was set to provide a spectral range of 4000–12500 cm⁻¹ with an 8 cm⁻¹ resolution. For model building, three NIR spectra were collected with 10 kHz scan speed and by averaging 32 scans from different locations of 36 samples, differing in apparent density, of both types of PET foams. The same settings were used for in-line sampling, except the in-line spectra were calculated from 16 scans to reduce sampling time.

SEM micrographs were obtained using EVO MA 10 instrument (Zeiss, Germany) at an accelerating voltage of 30 kV on specimens coated by 32 nm gold layer. The mean value and standard deviation of the diameter of the cell cross-sections approximated by a circle were determined from 250 to 400 measurements per sample.

Void fraction or porosity is defined as a fraction of the volume of voids over the total volume as a percentage. To determine the apparent density, porosity and expansion ratio of the foams, density measurements were performed by immersion method according to ASTM D792-13. Void fraction or porosity is defined as a fraction of the volume of voids over the total volume as a percentage. The percentage of void fraction (V_f) was calculated from apparent density (ρ_{app}) of foams and the density of the non-foamed extrudate (ρ) according to Equation (2):

$$V_f = 100\% * \left[1 - \left(\frac{\rho_{app}}{\rho}\right)\right] \tag{2}$$

Density (ρ) of the non-foamed PET based polymer mixtures were considered to be 1.375 g/cm³ (without talc) and 1.383 g/cm³ (with talc), while ρ_{app} of expanded samples was measured by Radwag AS 60/220.R2 analytical balance with density measurement kit in ethanol. The expansion ratio (Φ) was calculated according to Equation (3):

$$\varphi = \frac{\rho}{\rho_{app}} \tag{3}$$

Cell density (N_0) was determined based on Equation (4) [30]:

$$N_0 = \left(\frac{n}{A}\right)^{\frac{3}{2}} \varphi \tag{4}$$

where n is the number of cells in the SEM micrograph, and *A* is the area of the micrograph [cm^2].

The crystallization characteristics of rPET foam samples were determined with a DSC device type DSC131 EVO (Setaram, France). During non-isothermal crystallization, samples weighing 10–15 mg were heated to 320 °C at a rate of 20 °C/min and held there for 3 min to erase the thermal prehistory. Subsequent cooling was performed at a rate of 5–40 °C/min to −20 °C. The maximum value of exothermic peaks during cooling was considered to be the crystallization temperature.

3. Results and discussion

3.1. Improving the foamability of rPET

The molecular weight of the rPET was increased by reactive extrusion using 0.0–0.7% chain extender. The intrinsic viscosity value of the manufactured regranulates as a function of the chain extender content is shown in Fig. 1. It can be seen that without chain extender addition, the intrinsic viscosity value of rPET reduces to 0.62 dl/g due to the degradation during reprocessing by extrusion. To reach the initial intrinsic viscosity value of 0.73 dl/g approximately 0.5% chain extender is required. By using 0.7% chain extender, the intrinsic viscosity value of rPET increased to 0.87 dl/g, which value is still lower than the raw materials used for foaming in most previous experiments (see in Table 1). The increase in intrinsic viscosity observed with increasing chain extender content reveals an increase in the average molecular weight of PET chains [52]. Nevertheless, if melt strength proves to be satisfactory for successful foaming at lower additive content, this can be a cost-effective solution even for industrial implementation.

Besides the unmodified rPET, the rheological and thermal properties of two types of upgraded materials were analysed; one modified with 0.7% chain extender addition (rPET + 0.7% CE) and other also chain-extended with 0.7% additive but containing 1% talc as nucleating agent as well (rPET + 0.7% CE + 1% talc).
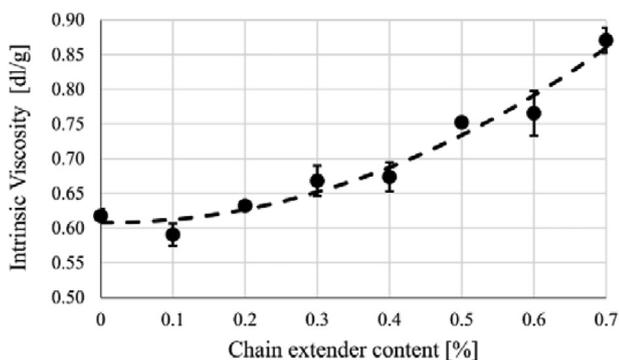
The viscosity curves of unmodified rPET and rPET modified with 0.7% chain extender with and without talc addition, as measured at 260 °C, are shown in Fig. 2. It can be seen that the viscosity curve of materials containing 0.7% chain extender shows a different character compared to unmodified rPET, which has a wide Newtonian plateau at low frequencies and is characterized by a slight shear thinning, suggesting a linear molecular structure. Materials containing chain extender, on the other hand, show noticeably increasing viscosity and pronounced shear thinning in the low frequency range as a result of the broader molar mass distribution and the introduced long-chain branches [53]. This behaviour is favourable during foaming to stabilize the cells. Talc was found to have little effect on the nature of the viscosity curve.

The additives used to improve foamability were expected to modify the crystallization behaviour of rPET and by this means to affect the process of cell wall solidification during foaming. The crystallization temperatures characterizing the solidification of the materials used were compared by non-isothermal crystallization at different cooling rates. It can be seen in Fig. 3 that the chain extender additive alone reduces the crystallization temperature of rPET as the long-chain branches inhibit the crystallization of the polymer. In contrast, talc increased the crystallization temperature of the chain extender containing material. Crystallization temperatures even higher than those of the unmodified rPET were measured in the entire cooling rate range tested. It was concluded that talc effectively acts as a crystal nucleating agent, and by hindering supercooling, it may facilitate faster solidification of the cell walls during cooling, which is of key importance regarding stabilization of the cellular structure.

3.2. Foam extrusion and characterisation

At the beginning of the foam extrusion process, sc-CO$_2$ with a constant volumetric rate of 0.5 mL/min was introduced into the barrel and mixed with the 260 °C melt. Then the resulting foam structure was stabilized by continuously lowering the melt temperature until the exiting product became highly expanded and uniform. The weight percentage of sc-CO$_2$ within the melt was measured to be 3.5 wt%, the plasticization effect of which was significant, since even if the material temperature was below 235 °C in the mold, the material still remained in molten state. The technological parameters characterizing the
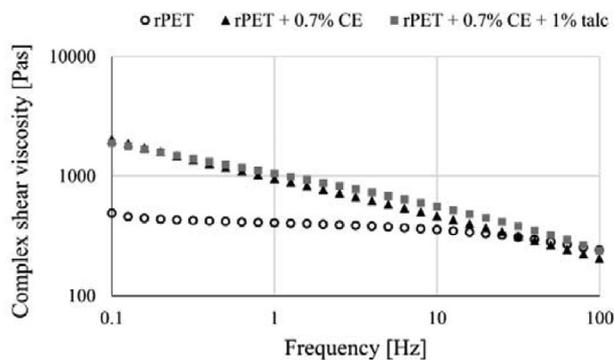
Fig. 1. Intrinsic viscosity value of regranulates produced by reactive extrusion as a function of chain extender content.

Fig. 2. Melt viscosity comparison of unmodified rPET, rPET with 0.7% CE and rPET with 0.7% CE + 1% talc (CE: Chain extender).

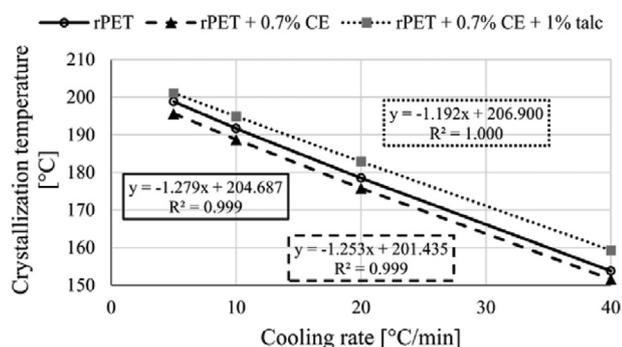**Fig. 3.** Crystallization temperature vs. cooling rate based on the non-isothermal crystallization measurements (CE: Chain extender).

Fig. 4. Photographs taken from a) unfoamed rPET; b) rPET + 0.7% CE foam; c) rPET + 0.7% CE + 1% talc foam (CE: Chain extender).

continuous production of highly expanded foams are shown in Table 2.

Fig. 4 compares the unfoamed extrudate prior to the introduction of sc-CO$_2$ and the foamed products made from the two selected modified materials. In both cases, outstandingly high porosity of 88—89% was reached accompanied with an expansion ratio of 8.6—9.2. These results outperform the published antecedents [41,48,49], especially when considering the cost-effectively achievable intrinsic viscosity value of 0.87 dl/g of the used material.

Samples were taken from the transition phase until stable conditions were reached and then characterised by SEM imaging, density measurements and Fourier transform NIR spectroscopy.

SEM images taken from the cross-sections of low-density (0.15—0.16 g/cm^3) foam samples obtained under steady state conditions, and of foam samples taken from the transition state with apparent densities ranging between 0.23 and 0.50 g/cm^3 are shown in Fig. 5. In each sample, an outer shell area of smaller cells and a core area of larger cells can be observed. There are two main reasons for the formation of this structure. On the one hand, the cooling rate is always higher at the cross-sectional edge, as a result of which cell growth is inhibited. On the other hand, at higher melt temperatures, the migration of gas into the environment is increased, which can cause cell collapse.

Analyzing the SEM images shown in Fig. 5, the average cell sizes and cell densities of the samples were calculated, the obtained results are shown in Fig. 6 as a function of apparent density. From foams with 0.7% chain extender but no talc, it can be observed that samples with a higher apparent density (0.30—0.50 g/cm^3), taken at higher die temperatures, have a noticeably higher average cell size and a lower cell density than those with lower apparent densities produced with colder die. This is consistent with the observation of Nikitine et al. [54] and Sameni et al. [55], who found that increasing die temperature
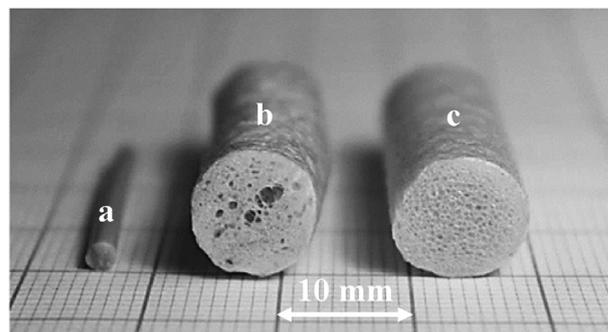
Table 2
Technological parameters of stationary extrusion foaming process.

Cylinder temp. zones [°C]	230—260
Screw speed [rpm]	25
Melt pump speed [rpm]	15
Melt pump temp. [°C]	240—245
Pressure before the melt pump [bar]	110—115
Temperature of static mixer [°C]	230—235
Temperature of die [°C]	230—235
Pressure at die [bar]	85—95
sc-CO$_2$ rate [mL/min %]	0.5
sc-CO$_2$ pressure [bar]	80—85

during extrusion foaming results in increasing cell size and decreasing cell density. It is assumed that fewer cell inductions occurred during homogeneous nucleation, and a significant number of fusions occurred during cell growth. For the raw material, which also contains talc, however, the average cell size and cell density do not show such a large difference between the samples with different apparent densities (Fig. 6). Since talc promotes not only heterogeneous cell nucleation but also crystallization, the cellular structure stabilizes more rapidly during the cooling process due to the beginning of solidification at higher temperatures (Fig. 3). The relative standard deviation of the cell diameters of the talc-containing samples is smaller (ranges between 39 and 43%) than that of the foams formed from homogeneous nucleation without talc (ranges between 44 and 71%), which indicates that a more uniform cellular structure is obtainable as a result of talc addition.

3.3. NIR signal-based quality monitoring

During the setting of the production parameters of highly expanded rPET foams, samples of different apparent densities were taken, the NIR spectrum of which was acquired off-line as an average of 3-3 measurement points using 32 scans. Prior to the chemometric evaluation, all spectra were normalized, smoothed, and the 1st derived spectra were evaluated in order to eliminate the intensity deviation between the measured points. The apparent density was estimated by partial least square (PLS) modelling using density measurement according to ASTM D792-13 as a reference method. The presence of talc affects the models, therefore different models were built for the samples containing and not containing talc. The number of Latent Variables (LVs) used in the models was optimized according to the R^2 values for calibration and cross-validation, and 3 LVs were selected for each models. The noticeable differences in the peak intensities and ratios provide a good basis for estimating the apparent density based on the NIR signal. As it can be seen in Fig. 7, there is a fairly good correlation between the density values estimated from the fitted model and the measured apparent density values for both talc-free and talc-containing rPET foam samples indicating the reliability of both models to be used for non-destructive density estimation. Somewhat higher correlation coefficient (R^2 = 0.911) was determined for the foams containing talc as nucleating agent, which is proposed to be attributed with the relatively constant, narrow ranges of cell density and average cell size (Fig. 6 a and b) of the analysed samples, and that no major structural change is observed in the examined range of apparent density (0.14—0.95 g/cm^3). The shell layer with differing

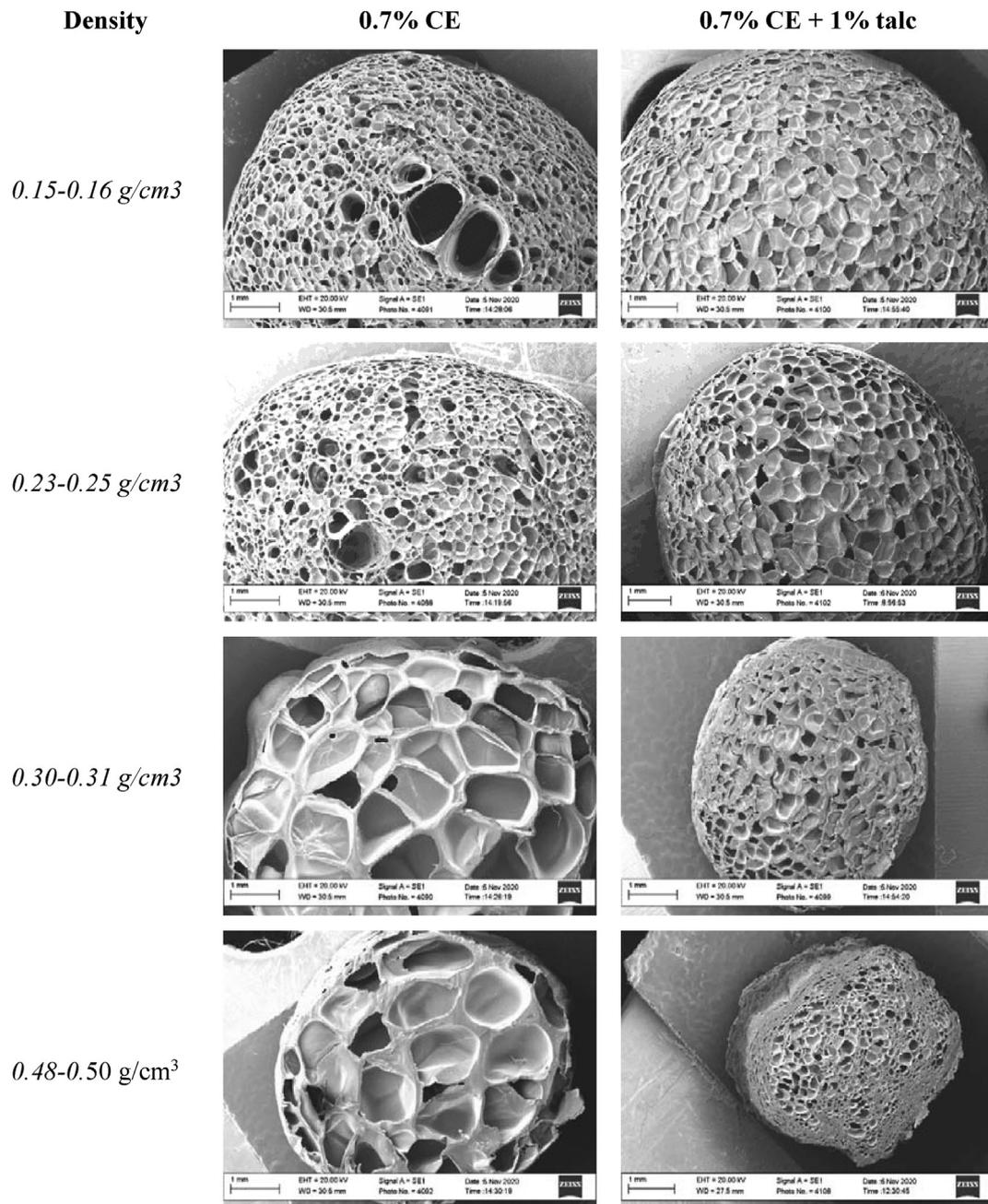| Density	0.7% CE	0.7% CE + 1% talc

Fig. 5. SEM images of rPET foam samples with different densities; left: with talc and right: without talc (CE: Chain extender).
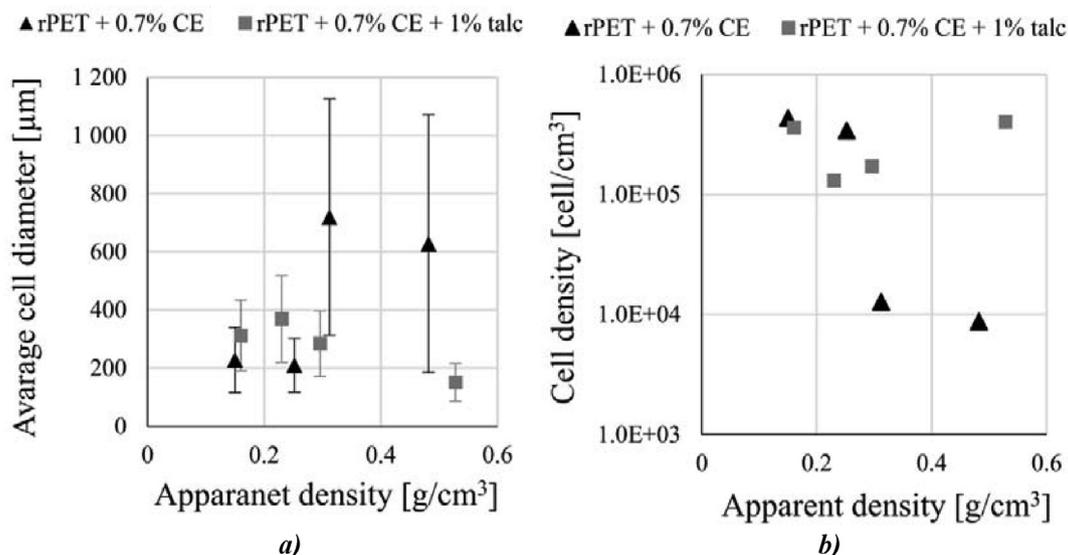
Fig. 6. Average cell diameter (a) and cell density (b) as a function of apparent density (CE: Chain extender).
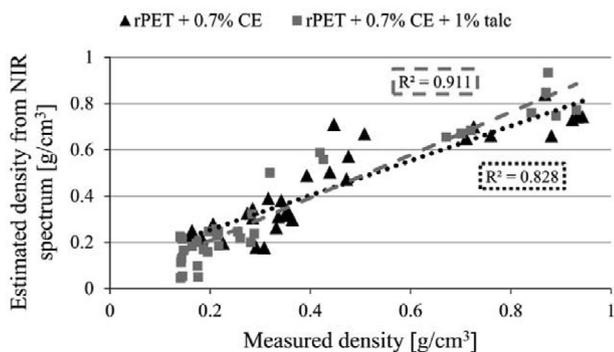

Fig. 7. Correlation between the measured and NIR signal based estimated density values (CE: Chain extender).

thickness and structure basically influence the penetration and scattering of NIR radiation, and therefore believed to be largely responsible for the detected error between the estimated and measured density values.

The applicability of NIR signal based in-line quality monitoring of rPET foaming is demonstrated by an experiment, where the density of the extrudate with 0.7% chain extender and 1% talc content was real-time analysed by multivariate data evaluation (PLS modelling) of the continuously recorded NIR spectra. For in-line monitoring, the measurement time was reduced by calculating the spectra from 16 scans instead of the 32 scans used for model building, therefore achieving spectra acquisition every 9 s. The setup used for in-line quality monitoring of foam extrusion is presented schematically in Fig. 8.

The density values estimated during the in-line NIR sampling of the extrudates and their moving average are shown in Fig. 9. Steady state production was disrupted 180 s after the NIR sensor was turned on by increasing the tool temperature, and in parallel, the structure and density of the produced foam also changed. The test section was sampled at 5 time points for validation purposes. The actual density values, obtained by immersion method (performed according to ASTM D792-13), are also indicated in Fig. 9. It can be stated that the density values estimated by PLS modelling of the NIR spectra continuously recorded from the extrudate show a good match with the validating apparent density values,
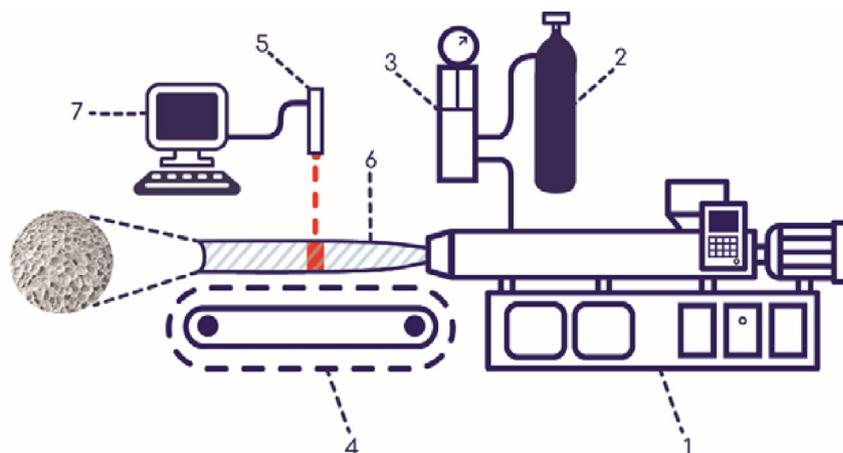

Fig. 8. Schematic drawing of foam extrusion with in-line quality monitoring system (1: extruder; 2: compressed CO_2 gas; 3: pump; 4: conveyor; 5: NIR sensor; 6: rPET foam; 7: data processing unit).
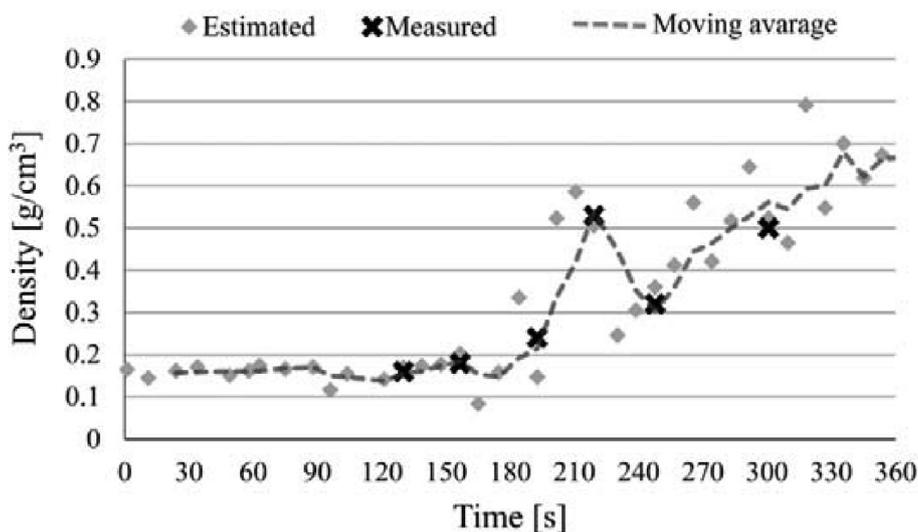
Fig. 9. Demonstration and validation of product's quality(density) change during continuous extrusion foaming.

therefore the method is assessed to be suitable for real-time quality monitoring of rPET foaming.

This is of great importance for industrial applicability, as the information obtained on the product's density can provide an opportunity for immediate intervention or regulation, thus providing an opportunity for a high level of quality assurance of the manufactured recycled foam product.

4. Conclusions

During our research, it was found that reactive extrusion of bottle grade PET regrind as starting material with 0.7% chain-extending additive can produce a raw material suitable for extrusion foaming. The intrinsic viscosity value of 0.86 dl/g proved to be adequate for stable and continuous production of highly expanded foams with apparent density lower than 0.15 g/cm^3.

It is presented that 1% addition of talc has a noticeable effect on both foam cell nucleation and PET crystallization. Heterogeneous nucleation increases cell induction, while crystallization at higher temperatures helps to stabilize small cells during cooling. As a result, the cellular structure of talc-containing foams become more uniform over a wide density range than that of the talc-free material. The proposed composition of starting material suitable for extrusion foaming requires minimal (less than <2%) additives, therefore it provides a cost-effective solution for the production of high-quality products even for industrial-scale implementation of recycling.

Utilizing the strong correlation evinced between the NIR spectrum and the apparent density of the rPET foams, the innovation of NIR spectrum based real-time quality monitoring is demonstrated. The proposed novel non-destructive, in-line applicable process contributes to the minimisation of production losses (wastrel) and is less time and human resource consuming than the commonly used procedures, and thus it can provide further cost savings. Similar spectroscopy-based quality control procedures are expected to gain application also in other fields where the constant physical or chemical structure of the products are important.

Declaration of competing interest

The authors declare no potential conflicts of interest with respect to the research, authorship, and/or publication of this article.

References

[1] A. Majumdar, S. Shukla, A.A. Singh, S. Arora, Circular fashion: properties of fabrics made from mechanically recycled poly-ethylene terephthalate (PET) bottles, Resour. Conserv. Recycl. 161 (2020) 104915, https://doi.org/10.1016/j.resconrec.2020.104915.
[2] H.B. Sharma, K.R. Vanapalli, V.S. Cheela, V.P. Ranjan, A.K. Jaglan, B. Dubey, S. Goel, J. Bhattacharya, Challenges, opportunities, and innovations for effective solid waste management during and post COVID-19 pandemic, Resour. Conserv. Recycl. 162 (2020) 105052, https://doi.org/10.1016/j.resconrec.2020.105052.
[3] N. Malik, P. Kumar, S. Shrivastava, S.B. Ghosh, An overview on PET waste recycling for application in packaging, Int. J. Plast. Technol. 21 (2017) 1–24, https://doi.org/10.1007/s12588-016-9164-1.
[4] I. Taniguchi, S. Yoshida, K. Hiraga, K. Miyamoto, Y. Kimura, K. Oda, Biodegradation of PET: current status and application aspects, ACS Catal. 9 (2019) 4089–4105, https://doi.org/10.1021/acscatal.8b05171.
[5] Y. Gu, G. Zhou, Y. Wu, M. Xu, T. Chang, Y. Gong, T. Zuo, Environmental performance analysis on resource multiple-life-cycle recycling system: evidence from waste pet bottles in China, Resour. Conserv. Recycl. 158 (2020) 104821, https://doi.org/10.1016/j.resconrec.2020.104821.
[6] T. Czigany, Disposable or single-use plastics? Neither! Recyclable or reusable plastics!, Express Polym. Lett. 14 (2020), https://doi.org/10.3144/expresspolymlett.2020.1, 1–1.

[7] Z. Zhang, C. Wang, K. Mai, Reinforcement of recycled PET for mechanical properties of isotactic polypropylene, Adv. Ind. Eng. Polym. Res. 2 (2019) 69–76, https://doi.org/10.1016/j.aiepr.2019.02.001.

[8] M. Edge, M. Hayes, M. Mohammadian, N.S. Allen, T.S. Jewitt, K. Brems, K. Jones, Aspects of poly(ethylene terephthalate) degradation for archival life and environmental degradation, Polym. Degrad. Stabil. 32 (1991) 131–153, https://doi.org/10.1016/0141-3910(91)90047-U.

[9] T. Abt, G. Álvarez, C. Rodríguez, M.L. Maspoch, Using the small punch test to analyse the influence of ultraviolet radiation on the mechanical behaviour of recycled polyethylene terephthalate, J. Strain Anal. Eng. Des. 54 (2019) 401–407, https://doi.org/10.1177/0309324719833237.

[10] G. Güçlü, T. Yalçinyuva, S. Özgümüş, M. Orbay, Hydrolysis of waste poly-ethylene terephthalate and characterization of products by differential scan-ning calorimetry, Thermochim. Acta 404 (2003) 193–205, https://doi.org/10.1016/S0040-6031(03)00160-6.

[11] J.D. Badía, F. Vilaplana, S. Karlsson, A. Ribes-Greus, Thermal analysis as a quality tool for assessing the influence of thermo-mechanical degradation on recycled poly(ethylene terephthalate), Polym. Test. 28 (2009) 169–175, https://doi.org/10.1016/j.polymertesting.2008.11.010.

[12] Y.J. Wang, S.C. Chen, S.S. Guang, Y. Wang, X.M. Zhang, W.X. Chen, Continuous post-polycondensation of high-viscosity poly(ethylene terephthalate) in the molten state, J. Appl. Polym. Sci. 136 (2019) 1–12, https://doi.org/10.1002/app.47484.

[13] A. Oromiehie, A. Mamizadeh, Recycling PET beverage bottles and improving properties, Polym. Int. 53 (2004) 728–732, https://doi.org/10.1002/pi.1389.

[14] S.A. Cruz, C.H. Scuracchio, L.B. Fitaroni, C. Oliveira, The use of melt rheology and solution viscometry for degradation study of post-consumer poly(-ethylene terephthalate): the effects of the contaminants, reprocessing and solid state polymerization, Polym. Test. 60 (2017), https://doi.org/10.1016/j.polymertesting.2017.03.026.

[15] F. Ronkay, T. Czigány, Development of composites with recycled PET matrix, Polym. Adv. Technol. 17 (2006) 830–834, https://doi.org/10.1002/pat.750.

[16] F. Alvarado Chacon, M.T. Brouwer, E.U. Thoden van Velzen, Effect of recycled content and rPET quality on the properties of PET bottles, part I: optical and mechanical properties, Packag. Technol. Sci. 33 (2020) 347–357, https://doi.org/10.1002/pts.2490.

[17] N.B. Sanches, M.L. Dias, E.B.A.V. Pacheco, Comparative techniques for molec-ular weight evaluation of poly(ethylene terephthalate) (PET), Polym. Test. 24 (2005) 688–693, https://doi.org/10.1016/j.polymertesting.2005.05.006.

[18] M. Asensio, K. Nuñez, J. Guerrero, M. Herrero, J.C. Merino, J.M. Pastor, Rheo-logical modification of recycled poly(ethylene terephthalate): blending and reactive extrusion, Polym. Degrad. Stabil. 179 (2020) 109258, https://doi.org/10.1016/j.polymdegradstab.2020.109258.

[19] H.-H. Yang, C.D. Han, The effect of nucleating agents on the foam extrusion characteristics, J. Appl. Polym. Sci. 29 (1984) 4465–4470, https://doi.org/10.1002/app.1984.070291281.

[20] J.S. Colton, N.P. Suh, The nucleation of microcellular thermoplastic foam with additives: Part II: experimental results and discussion, Polym. Eng. Sci. 27 (1987) 493–499, https://doi.org/10.1002/pen.760270703.

[21] S.N. Leung, C.B. Park, H. Li, Effects of nucleating agents shapes and interfacial properties on cell nucleation, J. Cell. Plast. 46 (2010) 441–460, https://doi.org/10.1177/0021955X10369418.

[22] W. Zhai, J. Yu, L. Wu, W. Ma, J. He, Heterogeneous nucleation uniformizing cell size distribution in microcellular nanocomposites foams, Polymer 47 (2006) 7580–7589, https://doi.org/10.1016/j.polymer.2006.08.034.

[23] D. Xu, H. Zhang, L. Pu, L. Li, Fabrication of Poly(vinylidene fluoride)/Multi-walled carbon nanotube nanocomposite foam via supercritical fluid carbon dioxide: synergistic enhancement of piezoelectric and mechanical properties, Compos. Sci. Technol. 192 (2020) 108108, https://doi.org/10.1016/j.compscitech.2020.108108.

[24] D. Klempner, V. Sendijarevic, Polymeric Foams and Foam Technology, Hanser Publishers, Munich, 2004.

[25] S. Suethao, D.U. Shah, W. Smitthipong, Recent progress in processing func-tionally graded polymer foams, Materials 13 (2020) 4060, https://doi.org/10.3390/ma13184060.

[26] Y. Ge, J. Lu, T. Liu, Analysis of bubble coalescence and determination of the bubble radius for long-chain branched poly(ethylene terephthalate) melt foaming with a pressure balanced bubble-growth model, AIChE J. 66 (2020), https://doi.org/10.1002/aic.16862.

[27] M. Xanthos, Q. Zhang, S.K. Dey, Y. Li, U. Yilmazer, M. O'Shea, Effects of resin rheology on the extrusion foaming characteristics of PET, J. Cell. Plast. 34 (1998) 498–510, https://doi.org/10.1177/0021955X9803400602.

[28] H. Yan, H. Yuan, F. Gao, L. Zhao, T. Liu, Modification of Poly(ethylene tere-phthalate) by combination of reactive extrusion and followed solid-state polycondensation for melt foaming, J. Appl. Polym. Sci. 132 (2015), https://doi.org/10.1002/app.42708 n/a-n/a.

[29] K. Bocz, B. Molnár, G. Marosi, F. Ronkay, Preparation of low-density micro-cellular foams from recycled PET modified by solid state polymerization and chain extension, J. Polym. Environ. 27 (2019) 343–351, https://doi.org/10.1007/s10924-018-1351-z.

[30] C. Fan, C. Wan, F. Gao, C. Huang, Z. Xi, Z. Xu, L. Zhao, T. Liu, Extrusion foaming of poly(ethylene terephthalate) with carbon dioxide based on rheology analysis, J. Cell. Plast. 52 (2016) 277–298, https://doi.org/10.1177/0021955X14566085.

[31] T. Nagata, M. Tanigaki, M. Ohshima, In-line NIR sensing of CO2 concentration in polymeric foaming extrusion process, J. Cell. Plast. 38 (2002) 11–30, https://doi.org/10.1106/002195502023187.

[32] T. Nagata, M. Tanigaki, M. Ohshima, On-line NIR sensing of CO2 concentration for polymer extrusion foaming processes, Polym. Eng. Sci. 40 (2000) 1843–1849, https://doi.org/10.1002/pen.11316.

[33] J. Tatiboue, R. Gendron, A. Hamel, A. Sahnoune, Effect of different nucleating agents on the degassing conditions as measured by ultrasonic sensors, J. Cell. Plast. 38 (2002) 203–218, https://doi.org/10.1177/0021955X02038003886.

[34] A. Sahnoune, J. TatibouËt, R. Gendron, A. Hamel, L. PichÉ, Application of ul-trasonic sensors in the study of physical foaming agents for foam extrusion, J. Cell. Plast. 37 (2001) 429–454, https://doi.org/10.1106/PEXL-PR2B-B1MH-47D3.

[35] A. Common, E. Rodier, M. Sauceau, J. Fages, Flow and mixing efficiency characterisation in a CO2-assisted single-screw extrusion process by resi-dence time distribution using Raman spectroscopy, Chem. Eng. Res. Des. 92 (2014) 1210–1218, https://doi.org/10.1016/j.cherd.2013.10.013.

[36] D.F. Baldwin, M. Shimbo, N.P. Suh, The role of gas dissolution and induced crystallization during microcellular polymer processing: a study of poly (ethylene terephthalate) and carbon dioxide systems, J. Eng. Mater. Technol. 117 (1995) 62–74, https://doi.org/10.1115/1.2804373.

[37] S. Japon, Y. Leterrier, J.A.E. Månson, Recycling of poly(ethylene terephthalate) into closed-cell foams, Polym. Eng. Sci. 40 (2000) 1942–1952, https://doi.org/10.1002/pen.11326.

[38] M. Xanthos, U. Yilmazer, J. Quintans, Melt viscoelasticity of polyethylene-terephthalate resins for low density extrusion foaming, Polym. Eng. Sci. 40 (2000) 554–566, https://doi.org/10.1002/pen.11186.

[39] R. Guan, B. Wang, D. Lu, Q. Fang, B. Xiang, Microcellular thin PET sheet foam preparation by compression molding, J. Appl. Polym. Sci. 93 (2004) 1698–1704, https://doi.org/10.1002/app.20614.

[40] L. Di Maio, I. Coccorullo, S. Montesano, L. Incarnato, Chain extension and foaming of recycled PET in extrusion equipment, Macromol. Symp. 228 (2005) 185–200, https://doi.org/10.1002/masy.200551017.

[41] I. Coccorullo, L. Di Maio, S. Montesano, L. Incarnato, Theoretical and experi-mental study of foaming process with chain extended recycled PET, Express Polym. Lett. 3 (2009) 84–96, https://doi.org/10.3144/expresspolymlett.2009.12.

[42] L. Sorrentino, E. Di Maio, S. Iannace, Poly(ethylene terephthalate) foams: correlation between the polymer properties and the foaming process, J. Appl. Polym. Sci. 116 (2010) 27–35, https://doi.org/10.1002/app.31427.

[43] T. Xia, Z. Xi, T. Liu, X. Pan, C. Fan, L. Zhao, Melt foamability of reactive extrusion-modified poly(ethylene terephthalate) with pyromellitic dianhy-dride using supercritical carbon dioxide as blowing agent, Polym. Eng. Sci. 55 (2014) 1528–1535, https://doi.org/10.1002/pen.23995.

[44] H. Liu, X. Wang, W. Liu, B. Liu, H. Zhou, Reactive modification of poly(ethylene terephthalate) and its foaming behavior, Cell. Polym. 33 (2014) 189–212.

[45] F. Ronkay, B. Molnár, G. Dogossy, The effect of mold temperature on chemical foaming of injection molded recycled polyethylene-terephthalate, Thermo-chim. Acta 651 (2017) 65–72, https://doi.org/10.1016/j.tca.2017.02.013.

[46] J. Li, S. Tang, Z. Wu, A. Zheng, Y. Guan, D. Wei, Branching and cross-linking of poly(ethylene terephthalate) and its foaming properties, Polym. Sci. B 59 (2017) 164–172, https://doi.org/10.1134/S1560090417020051.

[47] V.A. Szabó, G. Dogossy, Investigation of flame retardant rPET foam, Period. Polytech. - Mech. Eng. 64 (2019) 81–87, https://doi.org/10.3311/PPme.14556.

[48] C.-C. Lai, C.-T.T. Yu, F.-M.M. Wang, H.-T.T. Hsiao, W.-C.C. Liang, Y.-H.H. Ho, W.-F.F. Teng, L.-C.C. Liu, C.-M.M. Chen, Preparation of recycled polyethylene terephthalate composite foams and their feasible evaluation for electronic packages, Polym. Test. 74 (2019) 1–6, https://doi.org/10.1016/j.polymertesting.2018.12.009.

[49] S. Yao, D. Hu, Z. Xi, T. Liu, Z. Xu, L. Zhao, Effect of crystallization on tensile mechanical properties of PET foam: experiment and model prediction, Polym. Test. 90 (2020) 106649, https://doi.org/10.1016/j.polymertesting.2020.106649.

[50] Y. Zhao, Y. Li, D. Xie, J. Chen, Effect of chain extender on the compatibility, mechanical and gas barrier properties of poly(butylene adipate-co-tere-phthalate)/poly(propylene carbonate) bio-composites, J. Appl. Polym. Sci. (2021) 50487, https://doi.org/10.1002/app.50487.

[51] S.S. Karkhanis, L.M. Matuana, Extrusion blown films of poly (lactic acid) chain-extended with food grade multifunctional epoxies. https://doi.org/10.1002/pen.25224, 2019.

[52] F. Ronkay, B. Molnár, D. Nagy, G. Szarka, B. Iván, F. Kristály, V. Mertinger, K. Bocz, Melting temperature versus crystallinity: new way for identification and analysis of multiple endotherms of poly(ethylene terephthalate), J. Polym. Res. 27 (2020) 372, https://doi.org/10.1007/s10965-020-02327-7.

[53] M. Härth, A. Dörnhöfer, Film blowing of linear and long-chain branched poly(ethylene terephthalate), Polymers 12 (2020), https://doi.org/10.3390/polym12071605.

[54] C. Nikitine, E. Rodier, M. Sauceau, J.-J. Letourneau, J. Fages, Controlling the structure of a porous polymer by coupling supercritical CO 2 and single screw extrusion process, J. Appl. Polym. Sci. 115 (2010) 981–990, https://doi.org/10.1002/app.31031.

[55] J. Sameni, S.A. Jaffer, J. Tjong, W. Yang, M. Sain, Continuous foam extrusion of polyvinylidene fluoride (PVDF): chemical microfoam formation, Adv. Ind. Eng. Polym. Res. 3 (2020) 36–45, https://doi.org/10.1016/j.aiepr.2019.12.001.